

## Study on the effect of zinc oxide nanopowder doped with different concentrations of cobalt, on the properties of implants

N. M. Mihuț<sup>a,\*</sup>, A. M. Tătar<sup>a</sup>, M. M. Pasăre<sup>a</sup>, D. Cîrțînă<sup>a</sup>, C. Radulescu<sup>a</sup>,  
C. F. Ionici<sup>a</sup>, D. Păsculescu<sup>b</sup>, A Nioață<sup>a</sup>

<sup>a</sup>Constantin Brancuși University of Târgu-Jiu, Faculty of Engineering, 30 Eroilor st., 210135, Târgu-Jiu, Romania

<sup>b</sup>University of Petrosani, Faculty of Mechanical and Electrical Engineering, 20 University st., Petroșani, Romania

The aim of this study was to improve the physical, mechanical and chemical properties of biomaterials used in medical applications, by depositing thin films with superior properties on the surface of the materials. Starting from the antibacterial effect of ZnO nanopowders, doped or not with different concentrations of cobalt, five thermally treated thin films were deposited at 500°C, on a metallic titanium substrate, by the spin coating technique, a simple method that does not involve too many costs of depositing thin films on metal surfaces, starting from precursor liquids that gel over time. From the analysis of the resulting films, from a compositional, microstructural, morphological point of view, an increase in the antimicrobial activity of the materials used in implantology was found.

(Received October 5, 2022; Accepted January 19, 2023)

*Keywords:* Spin coating method, Thin films, Zinc oxide nanopowder, Cell tests

### 1. Introduction

Biomaterials have a long history, being used for about 50 years, without any knowledge of biocompatibility. Biocompatibility is defined as the property of a material to be compatible with living organisms, i.e. to be definitively accepted by the body without generating adverse reactions [1-4].

According to the specialized literature [5-6,], biomaterials represent natural or synthetic materials in contact or interaction with living organisms and biological fluids, with the aim of evaluating, treating, changing the shape or replacing any tissue, organ or function of the body. Even if a biomaterial can present all the physical, mechanical and chemical characteristics required by the medical application for which it is used, upon contact with biological environments and the human body, it finds particular physiological conditions with which it interacts through specific processes. Through these specific reactions that determine the degree of tolerance of the biomaterial by the host organism, the success of the medical act is ensured by the interaction between the biomaterial and the living organism, i.e. the biocompatibility of the material - biological environment [5, 7, 8].

The interaction between materials and the biological environment involves both the response of the living system to these materials (biocompatibility and bioactivity) and the response of the material to the living system (biodegradability). The introduction of the implant into the body requires it to have certain properties: mechanical resistance (to abrasion and fractures) and resistance to corrosion (to chemical dissolution and electrochemical corrosion) [9-10]. Moreover, the biomaterial and its possible degradation products must not be: responsible for inflammatory reactions, susceptible to the generation of allergic, toxic, mutagenic, carcinogenic reactions [2, 6]. A material that initially fulfills all the biocompatibility requirements may lose this property over time due to some processes of degradation, wear, fatigue, but also due to the aging or disease of the surrounding, initially healthy tissues [3, 11, 12, 13]. Specialized studies show that biomaterials with an anticorrosive composition and improved mechanical properties can be obtained by

---

\* Corresponding author: mihutnicoleta@gmail.com  
<https://doi.org/10.15251/DJNB.2023.181.117>

depositing thin films with superior properties on the surface of the materials used in the manufacture of indentations.

A thin film is defined as a dimensionally reduced material, created by the condensation of different atomic / molecular / ionic species of matter, having the same functionality as the initial bulk material and can vary depending on the destination of the respective layer from several tens to several hundreds of nanometers [10, 11, 14], improving wear resistance, corrosion resistance, optical properties, electrical and thermal properties, [15]. The deposition of thin films can be achieved using several methods, the most used being the chemical and physical ones: thermal spraying, coating by using plasma spraying, chemical vapor deposition, physical vapor deposition, deposition by the pulsed beam ablation method laser, vacuum plasma spraying, polymer replication method, Spin Coating method [6, 11, 16, 17].

The studies presented in this paper are based on the antibacterial effect of ZnO nanopowder doped or not doped with cobalt [18, 19], and aimed to obtain and characterize thin films of this type of nanopowder, in different concentrations, through the spin coating technique, starting from precursor liquids that gel over time.

An important problem for obtaining these thin layers was the choice of the composition of the deposited film, taking into account several factors such as: corrosion resistance, biocompatibility, the adhesion capacity between the film and the biomaterial, but above all the fact that the film must not influence negatively the properties of the biomaterial on which it is deposited, and as a deposition method we chose the Spin Coating method, because it is a simple method and does not involve too many costs.

The advantages of coating by the spin coating method are the simplicity and ease with which the process can be carried out, but also obtaining a thin and uniform film.

## **2. Experimental section**

### **2.1. Materials**

Thin layers of cobalt-doped or undoped zinc oxide nanopowders were obtained by the Spin Coating method, which generally consists of applying a thin, uniform film to the surface of a substrate by pouring a small amount of solutions of the desired material which extends over the entire surface on which it is deposited.

The samples on which the experiments were performed are thin films of Zinc oxide with and without Cobalt cation dopant deposited on a titanium support. To obtain them, we started from liquid precursor mixtures that gel over time using the sol-gel method.

The thin films of ZnO doped with  $\text{Co}^{2+}$  and undoped were obtained in the spin coating plant by going through the following steps:

- 1) the quantities of raw materials were dosed;
- 2) zinc acetate, cobalt sulfate, monoethanolamine and ethanol were mixed at  $60^{\circ}\text{C}$  on the hotplate with continuous stirring for 2 hours;
- 3) after 2 h the hydrolysis water was added; after approx. 1 min resulted in a white-opaque colloid for undoped Zinc oxide and different shades of purple for samples doped with Cobaltous cation (increasing the concentration of Cobaltous cation resulted in color intensification);
- 4) the layers were made by 5 depositions from the obtained solutions, each deposition consisting of 3 drops of solution; after each deposition, the samples were dried at a temperature of  $150^{\circ}\text{C}$  for 5 minutes, on a hot plate in order to evaporate the solvent, which according to literature data [32] must be done at an optimal temperature that allows obtaining the thickest possible film and uniform. The rotation speed was 1000rpm, the rotation time was 1 minute, and the rotation direction was clockwise.
- 5) after the deposition of the films, they were thermally treated at a temperature of  $500^{\circ}\text{C}$ , for 2 hours, in an oxidizing atmosphere.

To obtain the studied thin layers, the following materials were needed:

Table 1. Raw materials used to obtain masses based on ZnO.

Name of the substance	Formula	Manufacturing company	Characterization
Zinc acetate dihydrate	$(\text{ZnCH}_3\text{COO})_2 \cdot 2\text{H}_2\text{O}$	Sigma-Aldrich, Saint Luis, MI, SUA	$M = 219,51 \text{ g/mol}$ , $c = 99,9 \%$
Monoethanol amine	MEA $\text{H}_2\text{N}(\text{CH}_2\text{CH}_2\text{OH})$	Sigma-Aldrich, Saint Luis, MI, SUA	$\rho = 1,02 \text{ g/cm}^3$ , $M = 61,08 \text{ g/mol}$ , $c = 2 \%$
Absolute ethanol	$(\text{CH}_3)_2\text{CHOH}$	Sigma-Aldrich, Saint Luis, MI, SUA	$M = 46,07 \text{ g/mol}$ , $c = 99,8 \%$
Cobalt sulphate	$\text{CoSO}_4 \cdot 7\text{H}_2\text{O}$	Sigma-Aldrich, Saint Luis, MI, SUA	$M = 281,11 \text{ g/mol}$ , $c = 99,9 \%$
Zinc acetate dihydrate			

Cobalt sulfate heptahydrate was used for cobalt doping. Cobalt-doped zinc oxides were synthesized in various proportions: 0%, 0,5%, 1%, 1,5%, 2% și 5%. Molar ratio  $(\text{CH}_3\text{COO})_2\text{Zn}$ : MEA = 1: 2; alcohol: salts = 1: 2. Zinc acetate was dissolved in ethyl alcohol (~80%) under magnetic stirring at 60°C for about 30 min. After dissolving the salt, the monoethanol amine and the cobalt sulfate dissolved in the remaining alcohol were added. It was further stirred for approx. 2 h at 60°C after which the hydrolysis water was added. The result was a purple gel with different shades depending on the composition (increasing the dopant concentration led to color intensification).

Zinc oxide was doped with different concentrations of cobalt, and the results are presented in Table 2.

Table 2. Quantities of raw materials/precursors for the synthesis of 1 g ZnO doped with Co and undoped.

Sample code	Concentration $\text{Co}^{2+}$ [% mol]	$m_{\text{Zn}(\text{CH}_3\text{COO})_2 \cdot 2\text{H}_2\text{O}}$ [g]	$m_{\text{CoSO}_4 \cdot 7\text{H}_2\text{O}}$ [g]	$V_{\text{MEA}}$ [ $\text{cm}^3$ ]	$V_{(\text{CH}_3)_2\text{CHOH}}$ [ $\text{cm}^3$ ]
Z	0	2,69680	0	1,53	12,3
ZCo-0.5	0,5	2,6868	0,01717	1,47	12,24
ZCo-1	1	2,6771	0,03463	1,46	12,19
ZCo-1.5	1,5	2,66737	0,05199	1,456	12,15
ZCo-2	2	2,65750	0,06945	1,45	12,11
ZCo-5	5	2,59780	0,17511	1,42	11,83

Due to the remarkable properties and to achieve the objectives of the work, a titanium sheet grade 4 was used as a metal substrate, whose chemical composition is given in table 3 (max wt%, weight percentage).

Table 3. Chemical composition of the metal substrate.

Azote	Carbon	Hydrogen	Iron	Oxygen	Titanium
0,05	0,08	0,015	0,05	0,04	98,95

## 2.2. Methods

The analysis of the obtained materials was carried out through specific methods of solving the problem addressed. The resulting films were characterized from a compositional, microstructural and morphological point of view through different techniques, shown below:

a) X-ray diffraction. X-ray diffraction analysis was used to identify the crystalline mineralogical phases in the obtained films and obtain information on their degree of crystallinity. This was done with a Shimadzu XRD 6000 diffractometer with filtered radiation - Ni CuK $\alpha$  ( $\lambda = 1.5406 \text{ \AA}$ ), scanning speed from  $2^\circ/\text{min}$ , in the  $2\theta$  range of  $10\text{-}80^\circ$ .

b) Scanning electron microscopy. The microstructural and morpho-textural study of the deposited films was carried out using a scanning electron microscope Quanta INSPECT F.

c) RAMAN spectrometry. At the same time, in order to obtain detailed information regarding the polymorphism of the constituent phases of the studied films, the dispersive RAMAN spectroscopy technique was used. For this, the LabRAM HR Evolution spectroscopy from Horiba (Jobin Yvon) was used, equipped with a nitrogen-cooled detector, the source of which is an argon ion laser with a wavelength of 514 nm. Each measurement had an acquisition time of 180 seconds, and for each analysis the average of three measurements was made.

For the biological behavior, antimicrobial and hydrophobicity tests were carried out, as well as in-vitro tests on cell cultures (cell viability and oxidative stress).

d) Contact angle measurement. Through this technique, the angle formed at the intersection between the surface and the line representing the tangent to the drop of liquid on the surface is traced. The contact angle can be measured using an instrument called a goniometer. It performs a static measurement of the contact angles. A drop of water is deposited on the investigated surface, and the angle is measured either manually or with modern instruments. For values of the contact angle between 0 and 90, one can talk about the hydrophilic character of the surface, and values that exceed 90 describe a surface with a hydrophobic character. The device used to perform the contact angle analysis was Contact Angle Meter – KSV Instruments CAM 100.

e) Biofilm – functionalized solid material. To test the effect of the obtained surfaces on the production of biofilms, the materials were sterilized by exposure to UV radiation for 20 min on each side. A fragment of sterile material was deposited individually into a well of a sterile 24-well plate. On top of the deposited materials, 1 mL of liquid medium (simple broth) was added to the wells, followed by 50  $\mu\text{L}$  of 0.5 McFarland density microbial suspension. The plates with wells thus prepared were incubated at  $37^\circ\text{C}$  for 24h. After incubation the materials were washed with AFS (sterile physiological water) and the medium was changed, for the development of the biofilms developed on them. The plates were incubated for 24h). After the incubation period, the sample on which the biofilm had developed was washed with AFS and placed in a sterile tube in one mL of AFS. The tube was vigorously vortexed for 30 sec to detach the cells from the biofilm. The cell suspension obtained was diluted and different dilutions were seeded on plates with solidified culture medium in order to obtain and quantify the number of colony forming units (CFU/m).

f) Cell proliferation - MTT assay (Vybrant MTT cell Proliferation Assay kit, Molecular Probe). Based on this quantitative colorimetric method, it is possible to assess cell proliferation, viability and cytotoxicity. The method is based on the reduction of a yellow tetrazolium salt MTT (3-(4,5-dimethylthiazolium)-2,5-diphenyltetrazolium bromide) to dark blue formazan. Reduction by mitochondrial enzymes (especially succinate dehydrogenase) is an indication of cellular/mitochondrial integrity. Insoluble formazan can be solubilized with isopropanol, dimethylsulfoxide or other organic solvent. The optical density (OD) of the solubilized formazan is evaluated spectrophotometrically, obtaining an absorbance-dye concentration-number of metabolically active cells function in the culture. Cells are grown in 96-well plates at a seeding density of 3000 cells/well under different experimental conditions. Then 10  $\mu\text{L}$  12 mM MTT was added and incubated at  $37^\circ\text{C}$  for 4 hours. Then add 100  $\mu\text{L}$  of SDS-HCl solution, and pipette vigorously to solubilize the formazan crystals. Incubate for 1 hour, then pipette to homogenize and remove bubbles so as not to interfere with the reading. Read on a spectrophotometer at 570 nm (TECAN, Männedorf, Switzerland).

g) Working protocol for the assessment of oxidative stress (GSH-Glo™ Glutathione Assay, Promega). AFSC cells (mesenchymal stem cells isolated from amniotic fluid) are seeded at a density of 3000 cells in 300  $\mu\text{L}$  DMEM culture medium supplemented with 10% fetal bovine serum and 1% antibiotics (penicillin, streptomycin/neomycin) in 96-well plates. 24 hours after seeding, the cells are treated with biomaterials. Oxidative stress was assessed using the GSH-

Glo™ Glutathione Assay kit. This kit measures the amount of glutathione, an antioxidant agent. Glutathione produced by cells is converted by glutathione S-transferase to oxidized glutathione, the amount of glutathione converted being directly proportional to the amount of glutathione S-transferase enzyme that converts glutathione bound with a luciferin precursor to oxidized glutathione bound with light-emitting luciferin. The more intense the light, the more glutathione was converted, so more glutathione was synthesized, so the cell was more stressed. The working protocol consisted of adding 100  $\mu$ L 1X GSH-Glo™ Reagent and incubating at 37°C for 30 minutes. Then 100 $\mu$ l Luciferin Detection Reagent was added and incubated at 37°C for another 15 minutes. At the end of the 15 min, the medium in the wells with cells is well homogenized and then the plate is read on the luminometer.

h) Fluorescence microscopy. To highlight cell morphology and viability, cells were stained with a vital dye whose fluorescence is amplified after entering the cell, due to the action of cytosolic enzymes. AFSC cells (Mesenchymal stem cells isolated from amniotic fluid) are seeded at a density of 50,000 cells in 500  $\mu$ l of DMEM culture medium supplemented with 10% fetal bovine serum and 1% antibiotics (penicillin, streptomycin/neomycin) in 24-well plates. After 5 days after the addition of the biomaterial, the cells are stained with the RED CMTPIX fluorophore (Life Technologies, Invitrogen, USA), which is added to the culture medium (DMEM medium, Sigma-Aldrich, USA) at a final concentration of 5  $\mu$ M and incubate for 30 minutes to allow the dye to penetrate the cells. Cells are washed with PBS and visualized by fluorescence microscopy. Images were captured with a digital camera using Axio-Vision 4.6 software (Carl Zeiss, Germany).

### 3. Results and discussions

#### 3.1. X-RAY diffraction

This chapter highlights the results obtained from the analysis of the samples prepared by the methods described in the Materials and methods chapter. Figure 1 shows the X-ray diffraction of undoped and Co<sup>2+</sup>/Mg<sup>2+</sup>-doped ZnO thin layers obtained at 500 °C for 2 h. From the X-ray diffraction images shown in Figure 6, it can be seen that the main X-ray diffraction lines X recorded are characteristic of wurtzite type ZnO and the introduction of cobalt does not lead to the appearance of other diffraction interferences which suggests that the formation of other mineralogical phases does not occur.

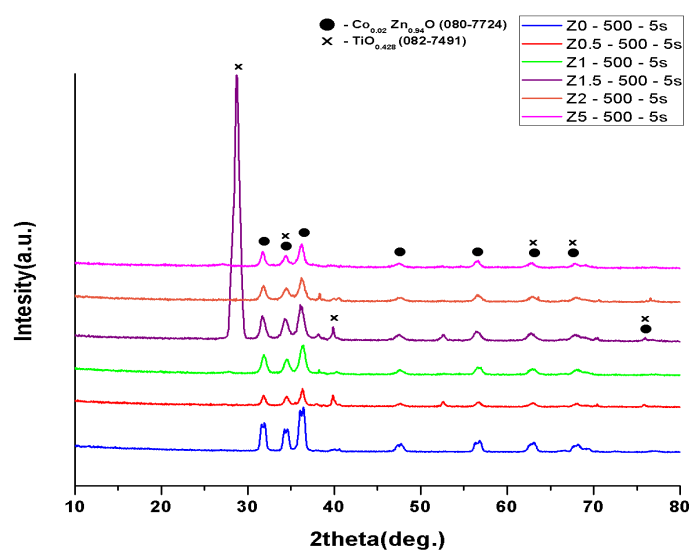


Fig. 1. X-ray diffraction of ZnO doped and undoped thin layers

Also, interferences characteristic of titanium or some forms of titanium dioxide have been highlighted, which denotes either a very small thickness of the film, or the existence of a non-uniform deposition of the film. The presence of TiO<sub>2</sub> films is explained by the fact that through the thermal treatment in an oxidizing atmosphere, titanium is passivated on the surface in an oxidic form. For the films obtained from 5 depositions, it is observed that solid solutions of the Zn<sub>1-x</sub>Co<sub>x</sub>O type are highlighted, where x can be 0.01 or 0.02. In order to obtain additional information regarding the influence of cobalt on the wurtzite ZnO structure, Raman determinations were made.

### 3.2. RAMAN spectrometry

The spectra of the Raman analyzes for the films deposited on the titanium substrate are represented in figure 2. From the analysis of the results, we noticed that bands characteristic of zinc oxide appear around the value of 440 cm<sup>-1</sup>. As the cobalt concentration increases, the intensity of these bands decreases.

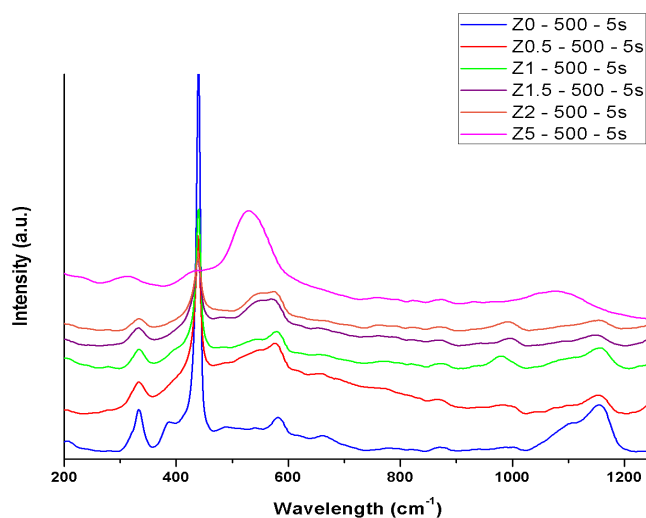


Fig. 2. Raman spectra of ZnO doped and undoped thin layers

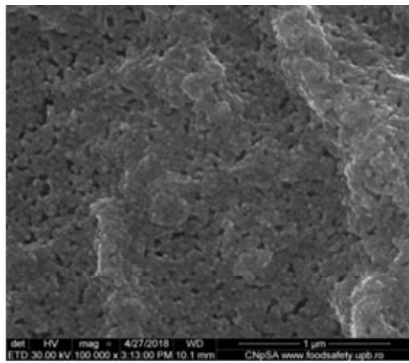
Also, the increase in intensity around the value of 580 cm<sup>-1</sup> is due to the increase in the cobalt content in the analyzed samples. This can be explained by the fact that cobalt ions distort the wurtzite structure of zinc oxide, which means that cobalt ions substitute zinc, results also obtained in other studies [17, 20].

When the concentration of cobalt increases, the band around the value of 440 cm<sup>-1</sup> disappears, which indicates that the incorporation of cobalt causes the disorder of the crystalline structure of the zinc oxide network but does not destroy its crystalline structure, an aspect that can also be observed in the XRD analyzes ( figure 1).

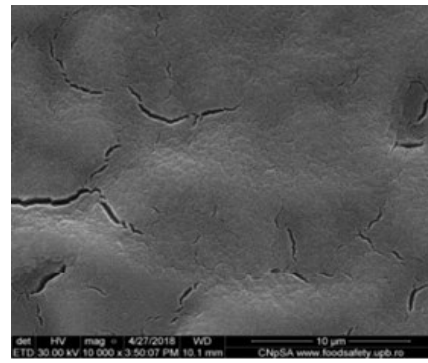
### 3.3. Scanning electron microscopy

To obtain information about the microstructural characteristics, surface quality/roughness and thickness of the deposited film, we used scanning electron spectrometry.

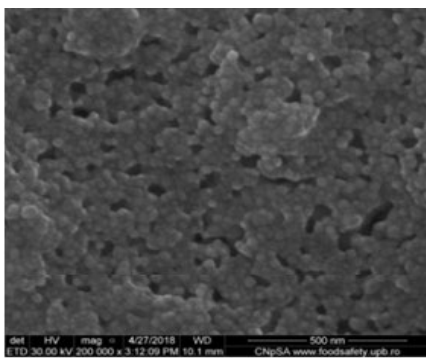
In figures 3 and 4 we presented the scanning electron microscopy images obtained for the thin films obtained by deposition using the spin-coating technique, for five depositions, thermally treated at 500°C, step 2 hours, and in figure 5 we observe the particle size distribution that make up the deposited thin films and the average particle size based on SEM images:



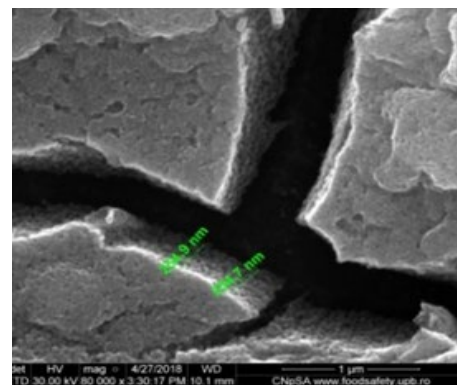
a) Z0-500-5s, h=255 nm, X20k



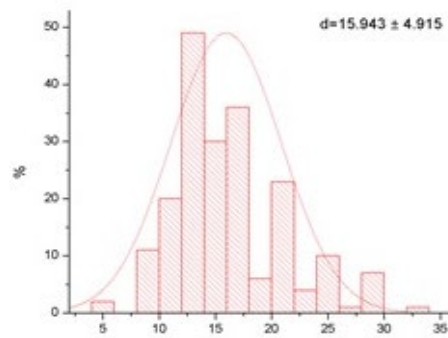
b) Z0-500-5s, h=255 nm, X100k



c) Z0-500-5s, h=255 nm, X200k

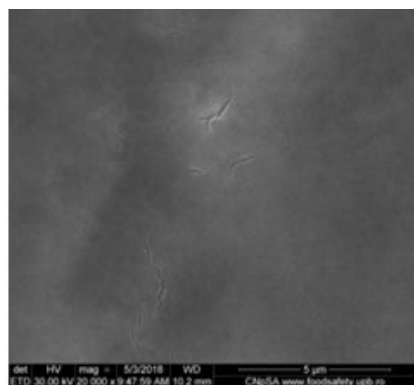


d) Z0-500-5s, h=255 nm

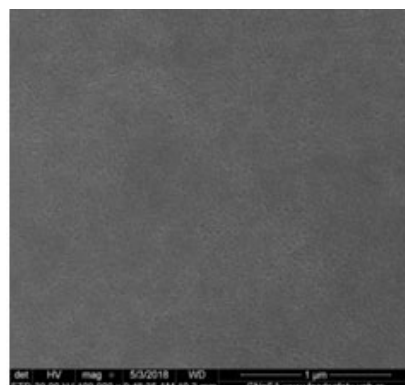


e) Particle size (nm)

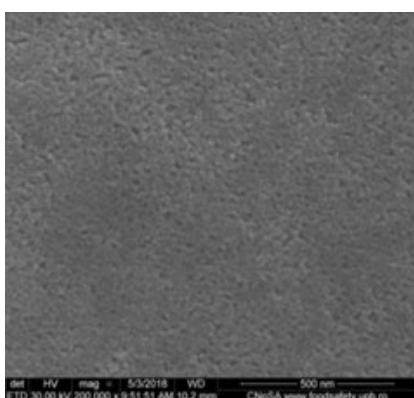
Fig. 3. Scanning electron microscopy images (a-d) and grain size distribution (e) for undoped ZnO thin films.



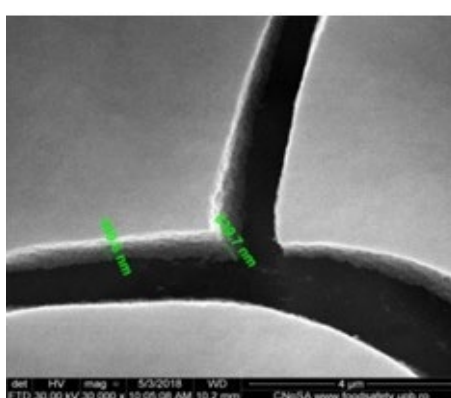
a) Z1,5-500-5s, h=545 nm, X20k



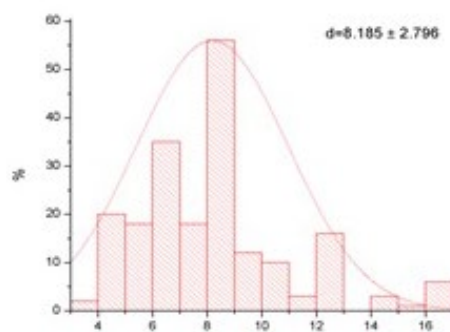
b) Z1,5-500-5s, h=545 nm, X100k



c) Z1,5-500-5s, h=545 nm, X200k

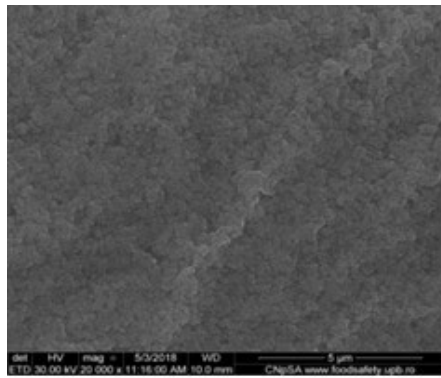


d) Z1,5-500-5s, h=545 nm

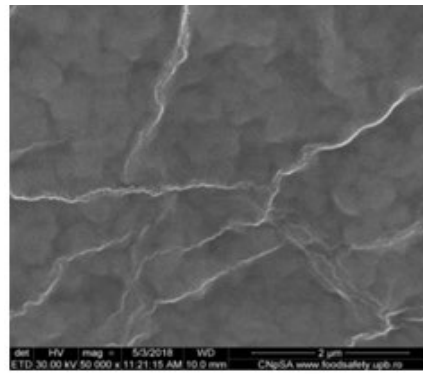


e) Particle size (nm)

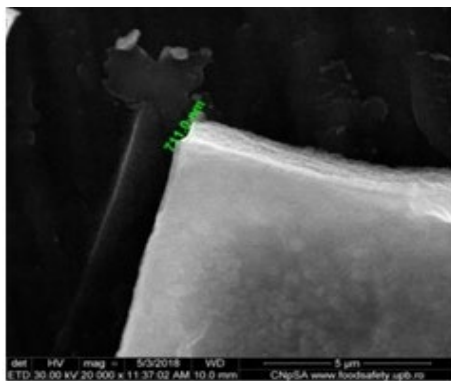
Fig. 4. Scanning electron microscopy images (a-d) and grain size distribution (e) for 1.5% Co<sup>2+</sup> doped ZnO thin films.



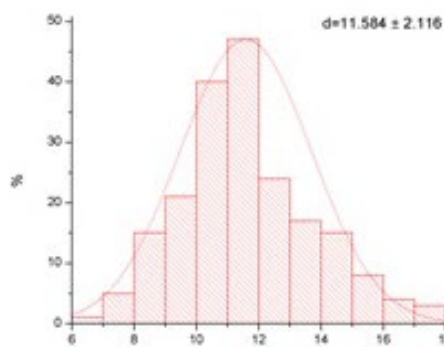
a) Z5-500-5s, h=710 nm, X20k



b) Z5-500-5s, h=710 nm, X100k



c) Z5-500-5s, h=710 nm



d) Particle size (nm)

Fig. 5. Scanning electron microscopy images (a-d) and grain size distribution (e) for 5% Co<sup>2+</sup> doped ZnO thin films.

Thus, from the scanning electron microscopy images presented in Figures 3 and 4, it is observed that, regardless of the number of depositions that led to the formation of the thin film, the doping of ZnO with cobalt leads to a denser microstructure, consisting of particles with morphology approx. spherical. When the dopant concentration increases, the microstructural density increases and the particle size, as a rule, decreases. Increasing the heat treatment temperature leads to an increase in the particle size. The SEM images also show us that the thin films are larger than 100 nm, with their thickness ranging from 130 nm to 870 nm. An influence of the dopant concentration and the heat treatment conditions on the film formation cannot be established, most likely due to the non-uniformity of the deposited film. Scanning electron microscopy images show us that the surface of the films is characterized by a nanometer-level roughness, which favors cell adhesion. Through the statistical processing of SEM images, we obtained information on the size distribution of the particles that make up the thin films, but also their variation with the change in the proportion of cobalt and the heat treatment temperature. From the analysis of the particle size distribution of the deposited thin films and of the average particle size based on the SEM images (Figures 3-e, 4-e and 5-e), it can be observed, in general, that the analyzed films have an approximately Gaussian size distribution of particles for the granules that make them up, and the statistical processing supports the statements made above. Scanning electron microscopy images show us that the surface of the films is characterized by a nanometer-level roughness, which favors cell adhesion.

### 3.4. Determination of the contact angle

When determining the contact angle, it can be observed that with the increase in the concentration of cobalt, there is a transition from the hydrophobic to the hydrophilic range, the results obtained being represented in figure 6. It can be deduced that the hydrophobicity of the deposited state increases with the increase in the number of deposits made. This is due to the increased concentration of zinc oxide.

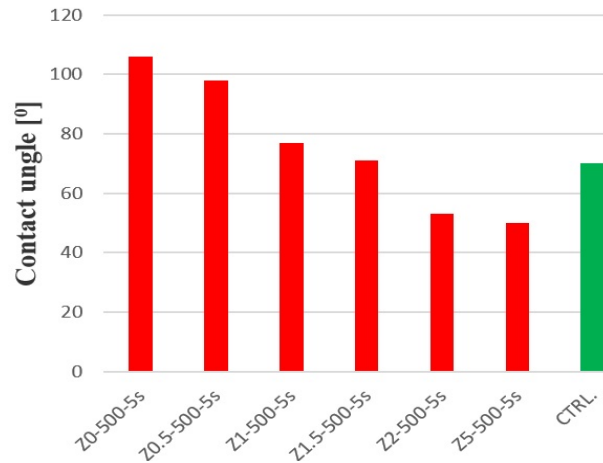


Fig. 6. The variation of the contact angle as a function of the cobalt concentration for the samples treated at 500°C

As far as bioadhesion is concerned, it can also be evaluated by the surface energy, which quantifies the excess energy from the surface of the material and which is closely related to the contact angle. This can be determined using relation 1.

$$\xi = \gamma \cos \Theta \quad (1)$$

where,  $\Theta$  - contact angle,  $\gamma$  - surface tension of water (72.8 mN/m)

Through the graphical representation of the obtained values, an increase in the surface energy was found with the decrease of the contact angle (Fig. 7). This supports the idea of a proportional increase in hydrophilicity with increasing cobalt concentration in the deposited layer.

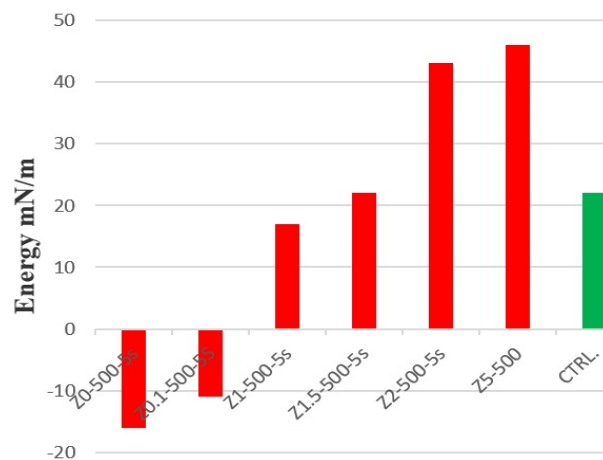


Fig. 7. Variation of surface energy as a function of cobalt concentration for samples treated at 500°C.

From figure 8 it can be seen that the films deposited by the spin coating technique show a very good antimicrobial activity against colonization and the formation of biofilms; the colonies formed per unit mL (UFC) being four orders of magnitude smaller than the uncoated titanium substrates or five orders of magnitude smaller than the control. Also, cobalt doping does not significantly affect the antimicrobial activity of ZnO.

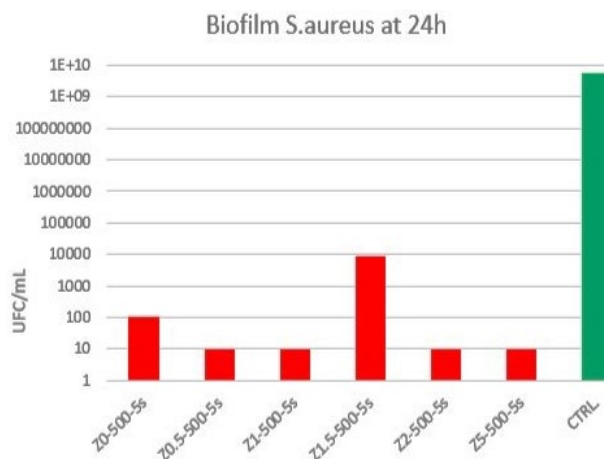


Fig. 8. *S.aureus* biofilm at 24 h = *S.aureus* biofilm at 24 h.

Even if the standard protocol does not mention keeping the samples in the medium for more than 72 hours, the obtained materials were kept for up to 7 days in the culture medium at normal temperature, which did not lead to the observation of the visible development of microorganisms, including microfungi (in general, after being kept in the nutrient culture medium, the emergence of contaminating microfungi is favored).

### 3.5. Cellular tests

The titanium alloy substrate oxidized on the surface by thermal treatment, as well as the thin films deposited on it by the spin coating technique, were characterized from an in-vitro point of view, also performing tests on cells, knowing from the specialized literature that ZnO in the form of nanopowder above a certain concentration has a toxic effect on cells [21]. In practice, cell viability and proliferation were monitored through these tests, through the cell proliferation test - MTT assay coupled with optical fluorescence microscopy, and the oxidative stress determined by these materials on AFSCs (mesenchymal stem cells isolated from amniotic fluid).

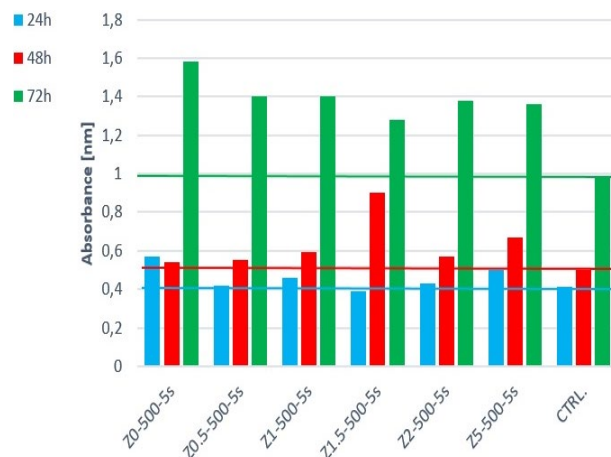
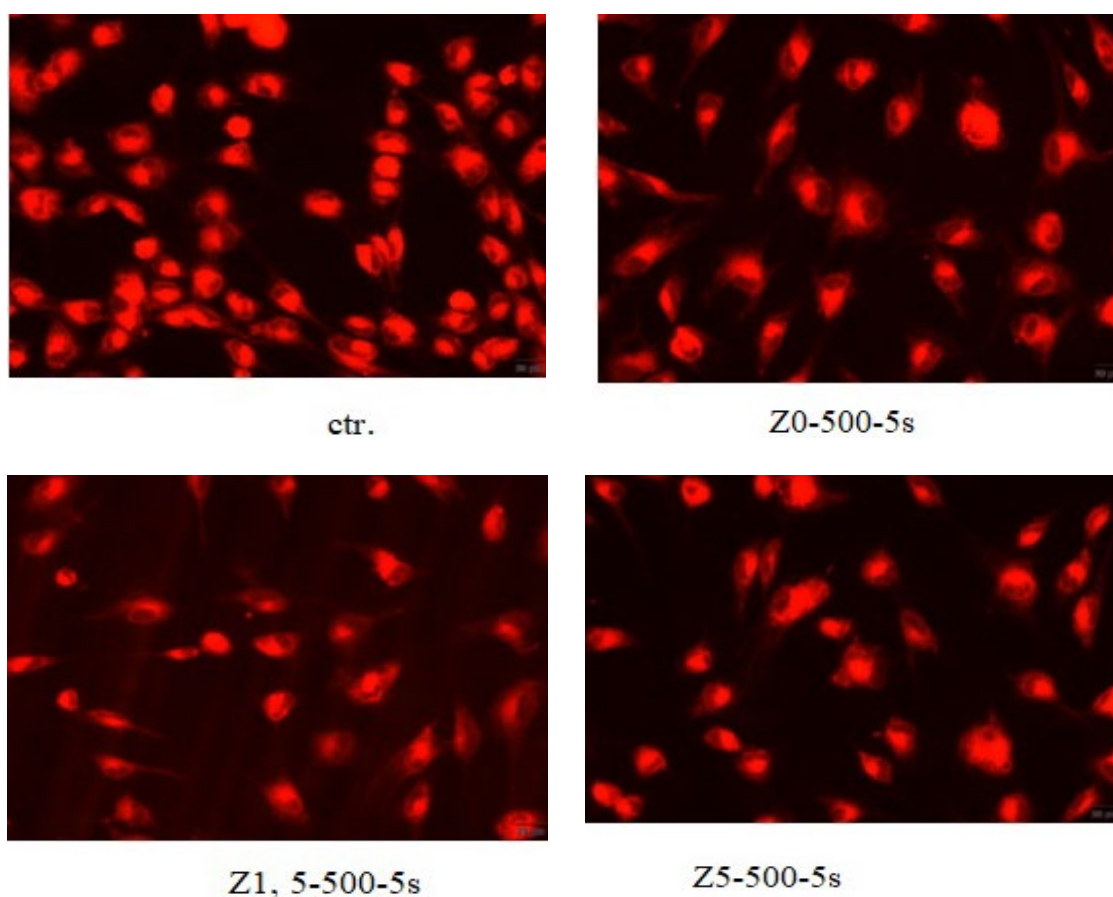


Fig. 9. Cytotoxicity tests on mesenchymal cells for the thin films obtained by deposition through the spin-coating technique, respectively five depositions, and thermally treated at 500°C, 2 hour step.

The films made from five depositions and thermally treated at 500°C were tested from the point of view of cell viability - Fig 9 and the results demonstrate that they had no cytotoxic effect, the absorbance values being close to or above those of the control sample. For samples Z0-500-5s and Z5-500-5s, a better proliferation is observed compared to the control at 24 hours (max. 62.81%). The films Z1.5-500-5s and Z5-500-5s stimulated the proliferation of AFSCs, the absorbance values being above those of the control sample at 48 hours (increases between 18.97-131.25%). At 72 hours, all the tested films stimulated cell metabolism, observing a significantly increased growth and proliferation compared to the control (increases between 48.09-71.12%).

The fluorescence optical microscopy images - Fig 10 and Fig. 11, shows that the cells are viable, the tested films having no cytotoxic effect, thus confirming the biochemical results. No dead cells or cellular debris are observed, AFSCs show a normal morphology, they have a characteristic fibroblast-like appearance, they emit extensions, which shows that they have an active phenotype. These extensions are possible due to the activity of the cytoskeleton, mainly actin filaments and microtubules. Cell metabolism is active, a fact shown by the fluorescence pictures, the cells incorporating the fluorescent CMTPX dye in the cytoplasm, which again suggests that the cells are viable.



*Fig. 10. Fluorescence optical microscopy for the thin films obtained by deposition using the spin-coating technique, respectively five depositions, and thermally treated at 500°C, 2 hour step.*

From Fig. 11 it is observed that at 24 hours in the presence of the films, the AFSC cells responded by increasing the expression of glutathione, a marker of oxidative stress; this increase can be attributed to an adaptation of the cells to the new culture medium.

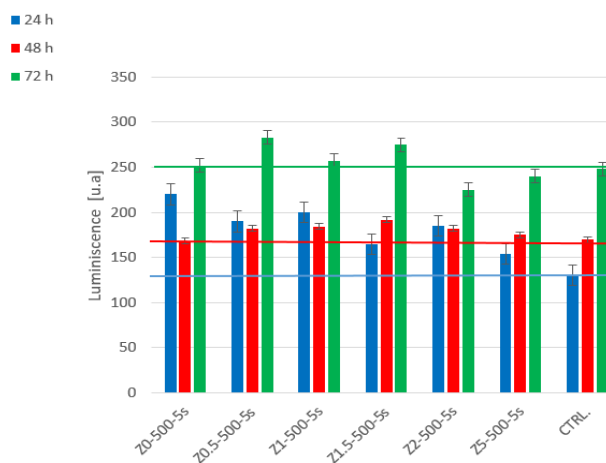


Fig. 11. Evaluation of oxidative stress by the GHS method on mesenchymal cells for the thin films obtained by deposition through the spin-coating technique, respectively five depositions, and thermally treated at 500°C, 2 hour step.

It is observed that at 48 and 72 hours, the level of glutathione is similar to that of control cells, which shows that AFSCs are not subjected to cellular stress. A slight increase in oxidative stress can be seen for Z1-500 and Z1.5-500 at 48 hours. At 72 hours increased values of oxidative stress were recorded for samples Z0.5-500 and Z1.5-500.

#### 4. Conclusions

The Spin Coating method is a simple and inexpensive method of depositing thin films on metal surfaces. Thus, using this method, thin films of pure zinc oxide but also doped with different concentrations of cobalt were successfully deposited, made up of 5 depositions and thermally treated at 500°C, on a metallic titanium substrate.

Analyzing the obtained experimental results, the following were found:

- regardless of the number of depositions that led to the formation of the thin film, doping ZnO with cobalt leads to a denser microstructure.

- when the dopant concentration increases, the microstructural density increases and the particle size decreases, regardless of the number of depositions that led to the formation of the thin film. Doping ZnO with cobalt leads to a denser microstructure, consisting of particles with an approximately spherical morphology.

- increasing the heat treatment temperature leads to an increase in the particle size. The particle size was observed to increase with increasing number of depositions leading to thin film formation. The SEM images also show us that the thin films are larger than 100 nm, with their thickness ranging from 130 nm to 870 nm. An influence of the dopant concentration and the heat treatment conditions on the film formation cannot be established, most likely due to the non-uniformity of the deposited film.

- the scanning electron microscopy images show us that the surface of the films is characterized by a roughness at the nanometric level, which favors cell adhesion

- from a microstructural point of view, the wurtzite type structure of zinc oxide was highlighted, noting that the introduction of cobalt does not determine the formation of mineralogical phases. Cobalt ions distort the structure of the zinc oxide structure but do not destroy it.

## Acknowledgments

The authors would like to thanks for Constantin Brancuși University of Târgu-Jiu, Faculty of Engineering, for the technical supports.

## References

- [1] Langer, R., Tirrell, D.A., *Nature*, 428(6982), 487, 2004; <https://doi.org/10.1038/nature02388>
- [2] Floroian, L., Badea, M., Șamotă, I., *Biomaterials with applications in medicine*, Brașov Medical Journal, Publishing House of Transilvania University of Brașov, 1, 14, 2015.
- [3] Popa. C., Șimion, V., ș.a., *Biomaterials Science - Metallic Biomaterials*. Cluj-Napoca U.T. Press, 278. 2008.
- [4] Karki, S., et al., *Asian Journal of Pharmaceutical Sciences*, 11(5), 574, 2016; <https://doi.org/10.1016/j.ajps.2016.05.004>
- [5] [www.tocilar.ro/chimie-general/biomateriale-proprietati-si-aplicatii-in-medicina-4021](http://www.tocilar.ro/chimie-general/biomateriale-proprietati-si-aplicatii-in-medicina-4021). [accessed on 04/05/2022, 19:53].
- [6] Pătrașcu, I., Ciocan, L.T., Miculescu, F., *Morpho-compositional study of the ageing biomaterial in bone implants*, *Journal of Optoelectronics and Advanced Materials*, 11(5), 744, 2009.
- [7] Pato, R.A., PhD Thesis, Technical University of Cluj Napoca. 12-32, 2011.
- [8] Linhua, XU., et al., *Tunable nanoporosity in Sr-doped ZnO thin films by thermal annealing treatment and its effect on photocatalytic activity*, *Journal of optoelectronics and advanced materials*, 19(1-2), 96, 2017.
- [9] Shuhua, D., Kejing, X., Juncheng L., Hongwei C., *Physica B: Condensed Matter*, 406(19), 3609, 2011; <https://doi.org/10.1016/j.physb.2011.06.053>
- [10] Brinker, C.J., *Journal of Non-Crystalline Solids*, 100(1), 31, 1988. Wasa, K., Kitabatake, M., Adachi, H., *Thin film materials technology: sputtering of control compound materials*, William Andrew Inc., 518, 2004; [https://doi.org/10.1016/0022-3093\(88\)90005-1](https://doi.org/10.1016/0022-3093(88)90005-1)
- [11] Wasa, K., Kitabatake, M., Adachi, H., *Thin film materials technology: sputtering of control compound materials*, William Andrew Inc., 518, 2004; <https://doi.org/10.1016/B978-081551483-1.50002-2>
- [12] Brandenburg, J., et al., *Applied Physics*, 79(4), 1005, 2004; <https://doi.org/10.1007/s00339-004-2615-0>
- [13] Jacob, A.A., et al., *Journal of Alloys and Compounds*, 695, 3753, 2017; <https://doi.org/10.1016/j.jallcom.2016.11.265>
- [14] Taylor, J.F., *Spin coating: An overview*, *Metal Finishing*, 99(1), 16, 2001; [https://doi.org/10.1016/S0026-0576\(01\)80527-4](https://doi.org/10.1016/S0026-0576(01)80527-4)
- [15] Znaidi, L., *Materials Science and Engineering: B*, 174(1), 18, 2010; <https://doi.org/10.1016/j.mseb.2010.07.001>
- [16] [www.ossila.com/pages/spin-coating](http://www.ossila.com/pages/spin-coating). [accessed on 17.04.2022, at 14:26].
- [17] Cao, Q., et al., *Current Applied Physics*, 14(5), 744, 2014; <https://doi.org/10.1016/j.cap.2014.03.011>
- [18] Zare, M., et al., *Journal of Materials Science & Technology*, 34(6), 1035, 2018; <https://doi.org/10.1016/j.jmst.2017.09.014>
- [19] Stoica, A.O., et al., *International Journal of Pharmaceutics*, 510(2), 430, 2016; <https://doi.org/10.1016/j.ijpharm.2015.09.043>
- [20] Acosta-Humánez, F., Almanza, O., Vargas, Hernandez, C., *Romanian Journal of Materials*, 45(4), 315, 2015.
- [21] Saranya, S., et al., *Toxicology Reports*, 4, 427, 2017; <https://doi.org/10.1016/j.toxrep.2017.07.005>